Electrical Power and Energy Systems 101 (2018) 103–115

Contents lists available at ScienceDirect

Electrical Power and Energy Systems

journal homepage: www.elsevier.com/locate/ijepes

A multiobjective hybrid bat algorithm for combined economic/emission dispatch

Huijun Liang[a], Yungang Liu[a,*], Fengzhong Li[a], Yanjun Shen[b]

[a] School of Control Science and Engineering, Shandong University, Jinan 250061, PR China
[b] College of Electrical Engineering & New Energy, China Three Gorges University, Yichang 443002, PR China

ARTICLE INFO

Keywords:
Multiobjective optimization
Economic/emission dispatch
Bat algorithm
Large-scale systems

ABSTRACT

In this paper, a multiobjective hybrid bat algorithm is proposed to solve the combined economic/emission dispatch problem with power flow constraints. In the proposed algorithm, an elitist nondominated sorting method and a modified crowding-distance sorting method are introduced to acquire an evenly distributed Pareto Optimal Front. A modified comprehensive learning strategy is used to enhance the learning ability of population. Through this way, each individual can learn not only from all individual best solutions but also from the global best solutions (nondominated solutions). A random black hole model is introduced to ensure that each dimension in current solution can be updated individually with a predefined probability. This is not only meaningful in enhancing the global search ability and accelerating convergence speed, but particularly key to deal with high dimensional systems, especially large-scale power systems. In addition, chaotic map is integrated to increase the diversity of population and avoid premature convergence. Finally, numerical examples on the IEEE 30-bus, 118-bus and 300-bus systems, are provided to demonstrate the superiority of the proposed algorithm.

1. Introduction

In power systems, the objective of economic dispatch problem is to seek an optimal schedule for all committed generators to minimize the operating fuel cost while satisfying all kinds of constraints such as load-demand balance constraint and generation capacity constraints [1,2]. However, with the increasing public concern on the environmental problem caused by fossil fuels, it is urgent for us not only to care for economic benefit, but also to tackle the emission problem of fossil fuels [3,4]. Therefore, the emission objective should also be involved.

1.1. Literature review and motivation

As a multiobjective optimization problem (MOP), the combined economic/emission dispatch (CEED) problem has been intensively studied by different technologies [3–18], which are mainly classified into two categories [19]:

(i) *Classical optimization methods* Such methods include linear programming [5], weighted sum method [6] and ε–constraints [7], etc. The most popular method among them is weighted sum method, which mainly has two drawbacks: ① This method, as well as other classical method, is not suitable for solving nonconvex and/or nonsmooth problems. ② Only one solution is generated in a single run, that is, if the Pareto Optimal Front (POF) has 100 non-dominated solutions, the program must be run 100 times by varying the weights [8,9].

(ii) *Evolutionary algorithm techniques* Many of these algorithms have been successfully introduced to solve the CEED problem, such as GA (genetic algorithm) based algorithm [1,12], PSO (particle swarm optimization) based algorithms [13,14], flower pollination algorithm [15], SMODE [16], FBHPSO-DE [17] and ant colony optimization [18]. These algorithms essentially remove the aforementioned drawbacks of weighted sum method, and are suitable to deal with the nonlinear and nonconvex optimization problem. However, it is well known that evolutionary algorithms have difficulty in dealing with premature convergence problem. For example, genetic algorithm (GA) often suffers from premature convergence problem once the degree of population diversity is sharply decreased [20], and PSO also encounters the same problem when particles trap into local optima [21,22]. Moreover, existing algorithms always have difficulties in dealing with large-scale system. For example, in PSO, all the dimensions of v_i^t or x_i^t are updated simultaneously rather than only for one dimension. In addition, the same parameters are

* Corresponding author.
E-mail address: lygfr@sdu.edu.cn (Y. Liu).

https://doi.org/10.1016/j.ijepes.2018.03.019
Received 27 November 2017; Received in revised form 9 March 2018; Accepted 15 March 2018
Available online 20 March 2018
0142-0615/

applied to the update of v_i^t and x_i^t in each step of iteration. These are harmful to enhance the diversity of v_i^t or x_i^t, and limit the performance of PSO especially for high dimensional systems.

As a promising evolutionary algorithm, bat algorithm (BA), proposed in [23], integrates the advantageous of PSO, harmony search and simulated annealing algorithm. Optimization problems about economic dispatch and CEED problem solved by BA have been reported in several literatures. For example, in [24], the economic dispatch problem was realized by chaotic BA, but it is a single objective optimization problem and does not include emission objective. In [25], BA was introduced to deal with the CEED problem, but the price penalty factor was used to convert the MOP to a single-optimization problem, so the POF could not be formed. In [26], a multiobjective BA (SALBA) was applied to dynamic environmental/economic dispatch problem. However, there are several drawbacks in the proposed algorithm: ① All the dimensions of each generated solution are updated simultaneously, that is, it cannot update each single dimension of a solution separately, which is very important for enhancing the global search ability of algorithm. ② The update for velocity, loudness and pulse emission is the same as original BA, which cannot be well suitable to MOP problem. As for the optimization model in [26], several important constraints are not included in the model such as voltage magnitude constraints and line flow constraints. In [27], the CEED problem was solved by BA, but the POF is generated by varying the weights of the two objectives and power flow constraints are not included in the CEED model. In [28], an improved BA was proposed to solve the CEED problem considering the uncertain of wind power, and the local random walk in original BA was replaced by mutation operator. However, it does not change the fact that all the dimensions in a solution are updated simultaneously, which would limit the performance of the proposed algorithm.

1.2. Contributions

In this paper, a **Multiobjective Hybrid Bat Algorithm** (MHBA) is proposed to solve the CEED problem including power flow constraints. The main contributions of this paper is listed as follows:

(i) *A new multiobjective hybrid bat algorithm (MHBA) is proposed, which is especially suitable for high dimensional systems.* The performance of MHBA is improved in the following aspects compared with the existing multiobjective BA in [25–29]. ① An elitist nondominated sorting method with external archive [30–32] is introduced to generate POF, which overcomes the drawbacks of weighted sum method. ② In order to increase the learning ability of population, the comprehensive learning strategy [38] is modified to update the velocity. ③ The random walk in original BA is replaced by the random black hole model proposed in [35]. This replacement is meaningful in enhancing the global search ability and accelerating convergence speed. More importantly, in MHBA, each dimension in current solution can be updated individually due to the replacement. This is essentially different from the original BA, and is key for MHBA to obtain better solutions for high dimensional systems compared with other algorithms. ④ To avoid premature convergence and increase the diversity of population, the loudness and pulse emission rate in multiobjective BA are replaced by chaotic map.

(ii) *The CEED of large-scale systems with power flow constraints are effectively solved by the proposed algorithm.* The integrating of random black hole model can greatly increase the random search efficiency, which make MHBA be more suitable for large-scale systems. The reason is given as follows: ① In MHBA, each dimension in current solution is updated individually with a probability p, and the update parameter is different for each step. This gives each individual the chance to alter the search direction in every iteration, and hence increases the diversity of solutions. But as for other algorithms, for example, PSO, all the dimensions in velocity v_i^t and position x_i^t are updated simultaneously with the same parameters in each iteration step. ② Each dimension in current solution not only can be absorbed by a black hole, but also can escape from the black hole because the speed of individuals is all remained in the process. This is meaningful in preventing premature convergence problem. ③ Different from the original random black hole model, the effective radius r_d in the model is treated as a piecewise parameter. This is helpful in enlarging search area for individuals at the beginning with a relatively large value of r_d, and improving the solution qualities with a relatively small value of r_d for the rest steps of iteration. The IEEE 118-bus system and IEEE 300-bus system are used in the simulation to demonstrate the effectiveness of the proposed algorithm in solving large-scale systems. The results show that RCBA has great advantages in dealing with the CEED of large-scale systems with power flow constraints compared with other algorithms.

The remainder of this paper is organized as follows. Section 2 describes the CEED problem including power flow constraints. Section 3 explores the approaches to improve the performance of BA for MOP and proposes the multiobjective optimization algorithm: MHBA. Section 4 gives the simulation results of the standard IEEE 30-bus system, IEEE 118-bus system and IEEE 300-bus system, and demonstrates the effectiveness of MHBA in dealing with the CEED of large-scale systems compared with other algorithms. Section 5 summarizes several conclusions and gives some future research directions.

2. Problem formulation

The CEED problem is aimed at minimizing fuel cost and emission simultaneously while satisfying various equality and inequality constraints. The objectives and constraints of CEED problem are formulated as follows.

2.1. Objectives

2.1.1. Objective 1: minimization of fuel cost

The total fuel cost including valve point effects is expressed as below [1]:

$$F(P) = \sum_{i=1}^{N} [a_i P_i^2 + b_i P_i + c_i + |d_i \sin(e_i(P_i^{\min} - P_i))|], \tag{1}$$

where N is the number of generators; $P = (P_1, P_2, \ldots, P_N)$;$P_i$ and $P_i^{\min}$ are the active power output and the minimum active power output limit of the i-th generator, respectively; $F(\cdot)$ is the total fuel cost; a_i, b_i, c_i, d_i and e_i are fuel cost coefficients of the i-th generator.

2.1.2. Objective 2: minimization of emission

The main emission caused by fossil fuels, such as nitrogen oxides (NO_x) and sulfur oxides (SO_x), is described as follow [9]:

$$E(P) = \sum_{i=1}^{N} [10^{-2}(\alpha_i P_i^2 + \beta_i P_i + \gamma_i) + \varepsilon_i \exp(\lambda_i P_i)], \tag{2}$$

where $E(\cdot)$ is the total emission; $\alpha_i, \beta_i, \gamma_i, \varepsilon_i$ and λ_i are emission coefficients of the i-th generator.

2.2. Constraints

2.2.1. Generation capacity constraints

The active power output P_i and reactive power output Q_i of the i-th generator should be restricted by lower and upper limits ($i = 1, \ldots, N$):

$$\begin{cases} P_i^{\min} \leqslant P_i \leqslant P_i^{\max}, \\ Q_i^{\min} \leqslant Q_i \leqslant Q_i^{\max}, \end{cases} \tag{3}$$

where $P_i^{\max}$ is the maximum active power output limit of the i-th generator; $Q_i^{\min}$ and $Q_i^{\max}$ are the minimum and maximum reactive power output limits of the i-th generator, respectively.

2.2.2. Power balance constraint

The total active power covers the total power load demand P_d and transmission line losses P_{loss}, which is described as:

$$\sum_{i=1}^{N} P_i = P_d + P_{\text{loss}}. \tag{4}$$

The transmission line losses are calculated by solving the following power flow equations [33,34,39]:

$$P_i - P_{di} - V_i \sum_{j=1}^{N_{\text{bus}}} V_j (G_{ij}\cos\theta_{ij} + B_{ij}\sin\theta_{ij}) = 0, \tag{5}$$

$$Q_i - Q_{di} - V_i \sum_{j=1}^{N_{\text{bus}}} V_j (G_{ij}\sin\theta_{ij} - B_{ij}\cos\theta_{ij}) = 0, \tag{6}$$

where P_{di} and Q_{di} are the active and reactive load demand at bus i, respectively; V_i and V_j are the voltage magnitudes at buses i and j, respectively; $\theta_{ij} = \theta_i - \theta_j$ (θ_i and θ_j are the voltage angles at buses i and j, respectively); G_{ij} and B_{ij} are the transfer conductance and susceptance between buses i and j, respectively; N_{bus} is the number of buses. After all the voltage magnitudes and angles are obtained, the real P_{loss} is calculated as

$$P_{\text{loss}} = \sum_{k=1}^{N_{\text{line}}} g_k [V_i^2 + V_j^2 - 2V_i V_j \cos\theta_{ij}], \tag{7}$$

where is the conductance of the k-th line connecting buses i and j; N_{line} is the number of transmission lines.

Most existing literatures on CEED do not consider power flow constraints [3,11,13,16–18]. This would result in the failure or mismatch when the methods are applied to practical systems. For example, reactive power, which is omitted in existing studies, may have great effect on active power and should be included in the research.

2.2.3. Voltage magnitude constraints

The voltage magnitude should be controlled between the lower and upper bounds for secure operation:

$$V_i^{\min} \leqslant V_i \leqslant V_i^{\max}, \quad i = 1,...,N_{\text{bus}}. \tag{8}$$

2.2.4. Line flow constraints

The security constraint of power for transmission line is restricted by

$$S_{ti} \leqslant S_{ti}^{\max}, i = 1,...,N_{\text{line}}, \tag{9}$$

where S_{ti} is the line flow at the i-th line, and $S_{ti}^{\max}$ is the upper limit line flow at the i-th line.

2.2.5. Ramp rate limits

The power output of units cannot change instantaneously, and is limited by the ramp rate limits:

$$\begin{cases} P_i - P_i^0 \leqslant UR_i, \\ P_i^0 - P_i \leqslant DR_i, \end{cases} \tag{10}$$

where UR_i and DR_i are the up ramp rate and down ramp rate limits of the i-th unit, respectively; P_i^0 is the previous output power.

2.2.6. Prohibited operating zones

Prohibited operating zones exist in thermal units due to the effect of shaft bearing, vibration of machines, etc. This would lead to discontinuous input-output characteristic curves which is described as follows:

$$\begin{cases} P_i^{\min} \leqslant P_i \leqslant P_{i,1}^L, \\ P_{i,k-1}^U \leqslant P_i \leqslant P_{i,k}^L, \\ P_{i,m}^U \leqslant P_i \leqslant P_i^{\max}, \end{cases} \tag{11}$$

where $k = 2,...,m; m$ is the number of POZs for the i-th thermal unit; $P_{i,m}^U$ and $P_{i,m}^L$ are the upper and lower limits of the m-th POZ for the i-th thermal unit, respectively.

3. The implementation of MHBA

This section is devoted to enhancing the performance of multiobjective BA and proposing the multiobjective optimization algorithm: MHBA.

3.1. Introduction of multiobjective bat algorithm

BA was first proposed in 2010 [23]. It simulates the behavior of bats hunting for prey. Based on the original BA, a multiobjective BA was proposed in [29]. According to [23,29], the frequency f_i, velocity v_i and position x_i of virtual bats are described as follows:

$$f_i = f_{\min} + (f_{\max} - f_{\min})\mu, \tag{12}$$

$$v_i^{t+1} = v_i^t + (x_i^t - x_b^t) f_i, \tag{13}$$

$$x_i^{t+1} = x_i^t + v_i^{t+1}, \tag{14}$$

where f_i is the frequency of pulse emitted by the i-th virtual bat; $\mu \in [0,1]$ is a random number with uniform distribution; $f_{\min}$ and $f_{\max}$ are the minimum and maximum frequency, respectively; v_i^t and x_i^t are the velocity and position of the i-th virtual bat at time step t, respectively; x_b^t is the global best position at time step t.

For local search, the random walk is defined to generate a new solution around the current best solution x_b^t, and is described as

$$x_i^{t+1,\text{new}} = x_b^t + \phi \hat{A}^t, \tag{15}$$

where $\hat{A}^t = (\sum_{i=1}^{N_p} A_i^t)/N_p$ is the average loudness at time step t (N_p is the number of population) and $\phi \in [0,1]$ is a random number. The pulse emission rate r_i and loudness A_i are updated as follows:

$$r_i^{t+1} = r_i^0 (1 - \exp(-\tau t)), \tag{16}$$

$$A_i^{t+1} = \xi A_i^t, \tag{17}$$

where $\tau \in (0,+\infty)$ and $\xi \in [0,1]$ are both constants.

In order to generate the POF, the weighted sum method is introduced in the existing multiobjective BA [29]. There are several drawbacks about this method:

(i) The weighted sum method is used, which works only for convex Pareto front and requires the program to be run as many times as the number of nondominated solutions in POF.
(ii) For a general MOP, POF is always needed, which is described by nondominated solutions. This means that all the nondominated solutions, rather than only one single global best solution, are optimal solutions. But for the update of velocity and random walk in [29], only one global optimal solution is needed. Therefore, the update for velocity (13) and random walk (15) are not suitable to MOP now.
(iii) The search ability of multiobjective BA completely depends on random walk (15). So the convergence speed slows down greatly if the algorithm traps into local optima. Moreover, all the dimensions of $x_i^{t+1,\text{new}}$ in (15) are updated simultaneously, that is, it cannot update each single dimension in $x_i^{t+1,\text{new}}$ separately, which is harmful to enhance the global search ability.
(iv) From the pseudo code in [29], we can see that the random walk will be executed and the new solutions will be accepted only when "rand > r_i" and "rand < A_i & $f(x_i) < f(x_*)$" are satisfied,

respectively. However, according to (16) and (17), $r_i \to r^0$ and $A_i \to 0$ as $t \to \infty$. Therefore, the chance for executing random walk and accepting new solutions is decreased greatly as the iteration going on, which has bad effect on increasing the diversity of population and avoiding premature convergence of BA.

3.2. Multiobjective hybrid bat algorithm: MHBA

Different strategies are introduced to overcome the above drawbacks and the pseudo code for MHBA is given in this subsection.

3.2.1. An elitist nondominated sorting method with external archive

To overcome the first drawback, an elitist strategy and nondominated sorting method are employed in generating the POF.

Definition 1 (*Pareto Dominance "≺"*). In a minimization MOP, let $F_i(x)$ denote the i-th objective function, $i \in \{1,...,n_f\}$. A feasible solution x' is said to dominate another feasible solution x'' (denoted by $x' \prec x''$) if and only if $F_i(x') \leqslant F_i(x'')$ for $\forall\, i \in \{1,...,n_f\}$ and $\exists\, i \in \{1,...,n_f\}$: $F_i(x') < F_i(x'')$.

In NSGA-II [37], an elitist nondominated sorting method was proposed. All the feasible solutions are employed to generate fronts with different ranks denoted by $\mathscr{F}_1,...,\mathscr{F}_{n_p}$ (n_p is the number of ranks), and the dominance relationship is $\mathscr{F}_1 \prec \mathscr{F}_2 \prec \mathscr{F}_3 ... \prec \mathscr{F}_{n_p}$. The new population for NSGA-II completely depends on the ranked fronts. Of course, the feasible solutions in $\mathscr{F}_1$ are chosen preferentially, but if the size of $\mathscr{F}_1$ is smaller than the number of population, solutions in $\mathscr{F}_2$ are selected next and so on.

Different from NSGA-II, in our algorithm, only the first nondominated set is generated, which is saved in the external archive as in [30–32]. This scheme is shown in Algorithm 1 (x_{non} denotes the new generated solution, S_{ea} denotes the nondominated solutions saved in external archive and "%" denotes comment).

Algorithm 1. Update scheme for external archive

```
Import data for x_non and S_ea
if x_non ≺ a set of members in S_ea then
    Delete these members from S_ea
    Add x_non to S_ea
else
    if Any member in S_ea ≺ x_non then
        Discard x_non
    else % nondominated with each other
        Add x_non to S_ea
    end if
end if
```

If the number of nondominated solutions in S_{ea} is larger than the predefined value, the crowding-distance sorting method is introduced to delete the redundant solutions. According to [37], the crowding-distances are calculated for all individuals, and then the nondominated solutions are listed in descending order by the crowding-distances. If the number of nondominated solutions is larger than the size of population N_p, the nondominated solutions ranked in top N_p are chosen and the rest are all deleted. For example, suppose that total ten nondominated solutions are obtained in Fig. 1(a) and only five of them are needed. The result is shown in Fig. 1(b) when the crowding-distance sorting method in [37] is used. In Fig. 1(b), the remained five nondominated solutions are not evenly distributed, because the solutions ranked in last five, i.e., $x_5,...,x_9$, are deleted simultaneously. The drawback of this method is that when one solution is deleted, it does not consider the influence on crowding-distance generated by its neighbors. In order to make up the deficiency, a modified crowding-distance sorting strategy [39] is introduced and shown in Algorithm 2.

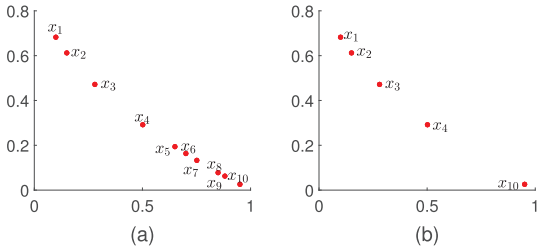

Fig. 1. (a) Demo exemplars; (b) crowding-distances sorting by NSGA-II 2.

Algorithm 2. The modified crowding-distance sorting strategy

```
Get the set of nondominated solutions
Get the number of the nondominated solutions which will be deleted (denoted by N_del)
while N_del > 0 do
    Calculate all the crowding-distances
    Delete the nondominated solution who has the smallest crowding-distance
    N_del = N_del−1
end while
```

With the strategy of Algorithm 2, only one nondominated solution is deleted in each iteration, and after this, the new crowding-distances will be calculated again. Fig. 2 shows the process with the same data in Fig. 1(a) by Algorithm 2. Only the nondominated solution with the smallest crowding-distance is deleted at each step. Therefore, a more evenly distribution along the Pareto front is obtained in Fig. 2(e) than that in Fig. 1(b).

3.2.2. A modified comprehensive learning strategy

To overcome the second drawback in Section 3.1, the comprehensive learning strategy in [38] is modified and then applied to the update of velocity (13).

In the original BA, the update of velocity depends on x_b^t, which is the only global best solution during the whole iteration. However, as stated previously, the set of best solutions for MOP, i.e., the POF, consists of many nondominated solutions rather than only one. So how to choose

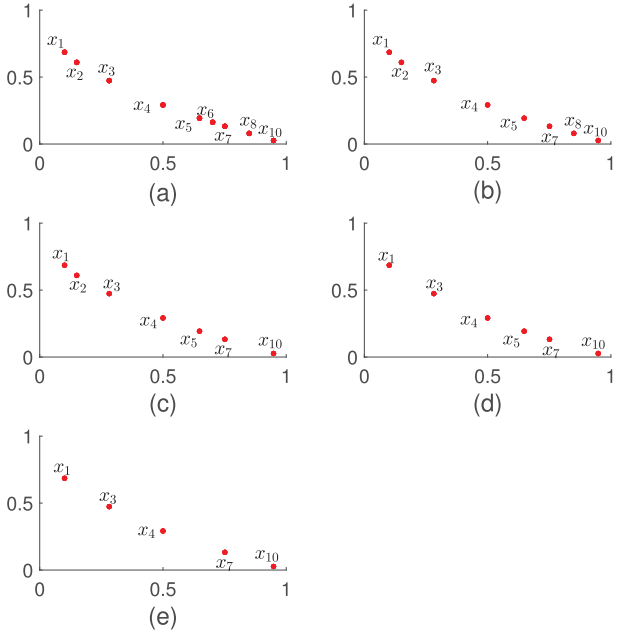

Fig. 2. The result using Algorithm 2: (a) x_9 is deleted; (b)x_6 is deleted; (c) x_8 is deleted; (d) x_2 is deleted; (e) x_5 is deleted.

the nondominated solutions is very crucial to MOP. At the same time, in (13), each individual only can learn from the global best solution and itself, but cannot learn from others. Therefore, another effective approach of enhancing the performance of BA is to share the information of other individuals.

In [38], a comprehensive learning strategy was proposed. Its main characteristic is that each dimension of a particle is capable of learning from different *pbests* (the best solution found by each particle) or the *gbest* (the global best solution).

Based on this idea, we form the following update rule for velocity v_i:

$$v_i^{t+1} = f_i(x_i^t - \text{gbest}_{\text{mop}}) + \omega_i v_i^t + c_1(1-\eta(i,:)) * (\text{pbest}_{fi} - v_i^t) r_1 + c_2 \eta(i,:)(\text{gbest}_{\text{mop}} - v_i^t) r_2, \quad (18)$$

where $\text{gbest}_{\text{mop}}$ is a randomly selected solution in $\mathscr{F}_1$;ω_i is the weighted coefficients; c_1 and c_2 are the acceleration constants; r_1 and r_2 are random numbers between 0 and 1; η is an $N_P \times N_n$ random matrix which consists of 0 and 1 (N_n is the dimension of MOP); pbest_{fi} is a compound solution whose dimensions are randomly selected in all *pbests* if $rand < P_c$, otherwise pbest_{fi} is the best solution found by the particle itself (*rand* is a random number between 0 and 1, and P_c is a predefined threshold value).

There are mainly two differences between (5) in [38] and (18):

(i) The frequency f_i is included in (18), which is suitable to BA.
(ii) In (18), each individual learns from pbest_{fi} and $\text{gbest}_{\text{mop}}$ simultaneously rather than learns from one of them.

By this means, each individual is able to learn not only from all individuals but also from the nondominated solutions, which is a significant step to enhance the learning ability of population.

3.2.3. The random black hole model

To overcome the third drawback in Section 3.1, the random walk (15) is replaced by the random black hole model [35].

According to [35], a random black hole is generated around the current *gbest* in each iteration of the algorithm. Each particle is regarded as a star and influenced by the gravity of generated black hole, which is treated as an approximate real solution because the real solution is kept unknown during the whole iteration process.

The schematic of random black hole model is shown in Fig. 3, where r_d is the radius of random black hole around *gbest*; gbest_n is the n-th dimension of *gbest*; $l \in [0,1]$ is a random value which denotes the attraction of random black hole to a star; $p \in [0,1]$ is a predefined threshold value; $x_{i,n}^{t+1}$ is the n-th dimension of x_i at time step $t+1$; the grey point x_i^t is the solution at time step t, and the blue point x_i^{t+1} is the solution at time step $t+1$ generated by (14). After the new solution x_i^{t+1} (the blue point) is generated, a new black hole (the red point) is formed around *gbest* (the yellow point), and the random number l associated with $x_{i,n}^{t+1}$ is generated. If $l \leqslant p$, the n-th dimension $x_{i,n}^{t+1}$ is captured by the black hole which is described as below:

$$x_{i,n}^{t+1} = \text{gbest}_n + r_d * \kappa, \quad (19)$$

where $\kappa \in [-1,+1]$ subjects to uniform distribution.

The above explanation is suitable to single objective optimization. In our algorithm, the *gbest* is randomly chosen from $\mathscr{F}_1$ for increasing the diversity of solution for MOP. Through this way, the global search ability of proposed algorithm can be greatly improved. The process for random black hole model is displayed in Algorithm 3.

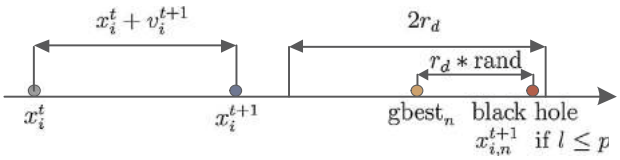

Fig. 3. The schematic of random black hole model.

Algorithm 3. The process for random black hole model

```
Randomly assign a value for gbest from F_1
for each dimension in x_i^{t+1} do
    Generate a random value for l
    if l ⩽ p then
        Update a dimension for x_i^{t+1} by (19)
    end if
end for
```

Algorithm 4. The pseudo code for MHBA

```
Initialize x_i, v_i, A_i, r_i, f_min, f_max, N_p and N_max
Initialize the parameters of comprehensive learning strategy
Get the fitness values according to x_i
Get nondominated solutions
while t < Max number of iterations do
    while j < N_p do
        Update pbest and gbest
        Update frequency, velocity and position by (12), (18) and (14)
        if rand > r_j then
            Run Algorithm 3 to update x_i
        end if
        Check constraints
        if rand < A_j then
            Accept new solutions
        end if
        Update r_j and A_j by (20)
    end while
    Calculate nondominated solutions
    Update external archive S_ea by Algorithm 1
    if the size of S_ea > N_max then
        Execute Algorithm 2
    end if
end while
Post process results and visualization
```

3.2.4. Chaotic map

In order to overcome the fourth drawback in Section 3.1, chaotic map is used. It is a powerful strategy for metaheuristic methods to increase the diversity of population and then avoid premature convergence by replacing random parameters or variables with chaotic sequences, which is helpful for algorithms to carry out overall searches [40–42]. For example, in [43], the pulse emission rate r and loudness A were both replaced by different chaotic maps, which brings better performance than the original BA.

In this paper, the tent map in [43] is adopted to replace the loudness A and pulse emission rate r simultaneously, which is defined as below:

$$u_{k+1} = \begin{cases} u_k/0.7 & \text{if } u_k < 0.7, \\ 10(1-u_k)/3 & \text{if } u_k \geqslant 0.7. \end{cases} \quad (20)$$

In this way, the chance for executing random walk and accepting new solutions is improved greatly, which is beneficial to avoid premature convergence.

3.2.5. The proposed MHBA

According to the above analysis, the multiobjective hybrid bat algorithm (MHBA) is proposed and the pseudo code is shown in Algorithm 4.

The main differences between MHBA and the existing multiobjective BA are listed as follows:

(i) The *pbest* and *gbest* are updated before executing (18) (see lines 7 and 8).
(ii) The random walk is replaced by the random black hole model, i.e., Algorithm 3 (see line 10).
(iii) The procedure "Accept new solutions" is executed only when $rand < A_j$ (see lines 13 and 14). The condition "$f(x_i) < f(x_*)$" (see line 12 in [29]), which is inappropriate to calculate Pareto dominance relationship, is deleted in this procedure.
(iv) Chaotic map is applied to the update of r_j and A_j (see line 16).
(v) The external archive and modified crowding-distance sorting strategy are introduced to obtain POF (see lines 19–22).

3.3. The parameter turning in MHBA

There are several parameters in MHBA. Among them, the most important parameters are c_1,c_2 (see (18)) and r_d. Parameters c_1 and c_2 determine the learning weight from the best solutions found by other individuals ($pbest_{fi}$) and nondominated solutions ($gbest_{mop}$). The value of r_d determines the search area of individuals. At the beginning of iteration, r_d should be assigned with a relatively big value for enlarging the search area because nearly all the random generated solutions are far away from the real solution (although it is unknown to us). But as iteration goes on, a relatively good solution is obtained, so the search area should be reduced. This means that r_d should be decreased.

In (12), the minimum value of frequency is always set to 0 [23,29], and the maximum value of frequency is determined by different systems. For the update of velocity v_i^t (see (18)), the weight coefficient ω_i which is in (0, 1), can be set to 0.5 at the initial stage; c_1 and c_2 should be adjusted with ω_i and r_d, and can be assigned a value in (0, 10) at the initial stage. Because ω_i is relatively fixed, the emphasis of parameter turning is focused on c_1,c_2 and r_d.

The following shows the parameter turning process. The effective radius r_d, which determines the search area of individuals, is the most important parameter in MHBA. At the initial stage, r_d can be assigned a value in (0, 10) generally. Then a simulation result would be generated. The value of r_d should be changed according to the result, and may exceed the range of (0, 10) determined by different systems. This process could be repeated several times until a relatively good result is obtained. Next, c_1 and c_2 would be modified with the same process. Three values (i.e., r_d,c_1 and c_2) are obtained after the two processes. If the simulation result is acceptable, the process of parameter turning is finished. Otherwise, the above two steps should be repeated until a satisfying result occurs.

Algorithm 5. The process for dealing with equality constraint

1: Acquire solution P = $\{P_1,...,P_N\}$
2: If the index of slack bus is not 1, exchange the slack bus with P_1
3: Let $P_{loss} = 0$, calculate the error by (4) (i.e., $|P_d - \sum_{i=1}^{N} P_i|$)
4: **if** error $> P_1^{max}$ or error $< P_1^{min}$ **then**
5: **if** error $> P_1^{max}$ **then**
6: $P_1 = P_1^{max}/3$
7: Assign power to $\{P_2,...,P_N\}$ with their maximum capacity one by one until the remained power is satisfied
8: **end if**
9: **if** error $< P_1^{min}$ **then**
10: $P_1 = P_1^{min}$
11: Assign power to $\{P_2,...,P_N\}$ with their minimum capacity one by one until the remained power is satisfied
12: **end if**
13: **end if**
14: Put the slack bus back to its original place

3.4. Implement MHBA to CEED problem

Special attentions should be paid to several steps in Algorithm 4 for applying MHBA to CEED problem:

(i) When initializing x_i, the value of x_i subjects to not only the inequality (3) but also the equality (4). If (4) is not satisfied, the solutions with initialized x_i may be very small, which is likely to dominate any other solutions generated by the whole iteration in Algorithm 4. This will fail to obtain the POF. Algorithm 5 gives the detailed steps for dealing with equality constraint. In the third step, P_{loss} is set to 0 because the losses are calculated by MATPOWER.
(ii) For the 12th line in Algorithm 4, constraints (3)–(10) are all satisfied by the usage of MATPOWER [36], and constraint (11) is realized by Matlab program.
(iii) Parameters in Algorithm 4 should be adjusted according to different scenarios in order to acquire better performance.
(iv) The fuzzy set theory is introduced to get the best compromise solution. Interested readers are referred to [46] for details.

4. Examples and results

In this paper, the units of active power, cost, emission and run time are MW, $/h, ton/h and second (s), respectively. The "run time" in the following tables represents the consumed time for the run which obtains the best fuel cost shown in each table.

4.1. Case 1: simulation for the standard IEEE 30-bus system

The CEED problem is solved by the proposed MHBA on the standard IEEE 30-bus 6-generator system. The parameters of generator fuel cost and emission come from [14]. The number of population for MHBA is 40. The parameter r_d and threshold p for the random black hole model are 0.01 and 0.5, respectively, and the learning probability P_c is 0.1. The total load demand is 283.4 MW. To compare the performance with other works, this case does not include valve point effects.

In this case, total 100 nondominated solutions are generated as shown in Fig. 4. The two extreme solutions are (607.39, 0.220857) and (643.376, 0.194209), respectively. We can see the obtained nondominated solutions well depict the POF of the CEED problem with IEEE 30-bus system. The comparison results with other algorithms are shown in Tables 1 and 2.

Table 1 shows the comparison results of the best fuel cost for IEEE 30-bus system with different algorithms. Among the algorithms, MHBA obtains the smallest value of fuel cost (i.e., 607.3900$/h), which is

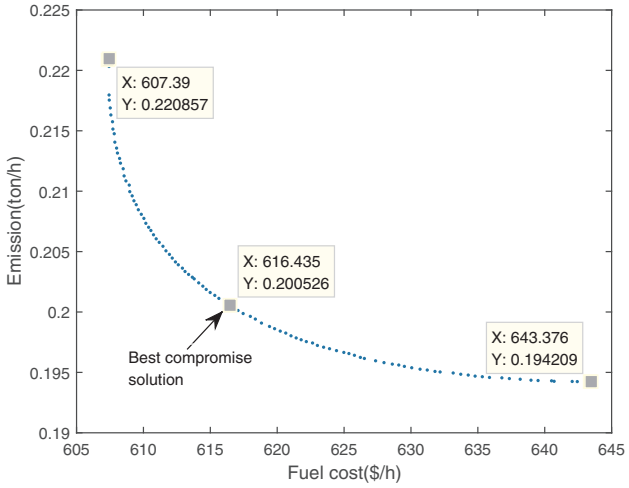

Fig. 4. Simulation result for case 1 with MHBA.

Table 1
Best solutions of fuel cost for case 1 (Power: MW, Cost: $/h, Emission: ton/h, Run time: s).

Items	MHBA	FSBF [34]	NSBF [34]	NSGA-II + DCD [45]	NSGA-II + DCD + CE [45]
P_1	10.94	19.43	17.80	11.44	11.44
P_2	29.85	37.26	33.66	30.29	30.57
P_3	58.29	68.57	72.92	60.43	59.84
P_4	99.48	59.19	59.08	97.95	98.02
P_5	51.81	60.85	57.66	51.56	51.52
P_6	36.20	40.61	44.74	35.18	35.46
Loss	3.204	2.51	2.46	3.45	3.47
Cost	**607.3900**	619.3679	619.6086	608.1283	608.1247
Emission	0.2208	0.2015	0.2027	0.2199	0.2198
Run time	**74.6098**	181.721	208.965	–	–

Table 2
Best solutions of emission for case 1 (Power: MW, Cost: $/h, Emission: ton/h).

Items	MHBA	FSBF [34]	NSBF [34]	NSGA-II + DCD [45]	NSGA-II + DCD + CE [45]
P_1	40.94	41.19	40.47	41.00	41.02
P_2	45.15	46.62	45.33	46.10	46.16
P_3	53.30	54.21	54.39	55.28	54.46
P_4	40.51	38.48	39.21	38.94	39.00
P_5	54.25	54.31	54.54	54.46	54.48
P_6	52.14	51.60	52.46	50.88	51.57
Loss	2.92	3.01	3.00	3.28	3.31
Cost	643.3760	645.6193	644.4141	645.3998	645.6472
Emission	**0.1942**	**0.1942**	**0.1942**	**0.1942**	**0.1942**

much superior to the values obtained by FSBF and NSBF. The difference of the values between MHBA and FSBF/NSBF is about 12$/h, which means a great savings (about 100000 $) in a year. MHBA also outperforms NSGA-II + DCD and NSGA-II + DCD + CE in terms of the best fuel cost. Table 2 show the best values of emission for this case. It can be seen that all the five algorithms have nearly the same best value of emission. From the above comparison, a better solution is achieved by MHBA.

As for the comparison of run time, RCBA has overwhelming advantage in the listed algorithms. From the last line of Table 1, the run time for generating the 100 nondominated solutions is about 74.609 s, which is much smaller than the consumed time of other algorithms. Thanks for the integrating of random black hole model and chaotic map, the proposed MHBA can have such better performance.

To further disclose the superiority of RCBA, a statistical results for the two values (i.e., the best solution of cost and emission) with ten runs are provided in Table 3. The maximum, minimum and average value of best cost by MHBA are 607.5692$/h, 607.3897$/h and 607.4492$/h, respectively. All these values are smaller than the corresponding values obtained by the other listed algorithms in Table 1. As for the best emissions, the four algorithms have nearly the same value, i.e., 0.1942 ton/h. It should be pointed out that, in [45], the objective function of emission is defined as:

Table 3
Statistical results for the best fuel cost and emission with ten runs for case 1 (Cost: $/h, Emission: ton/h).

Algorithm	Items	Maximum	Minimum	Average
MHBA	Best cost	607.5692	607.3897	607.4492
	Best emission	0.1942	0.1942	0.1942
NSGA-II [45]	Best cost	–	608.13	–
	Best emission	–	0.1942	–
NSGA-II + DCD [45]	Best cost	–	608.13	–
	Best emission	–	0.1942	–
NSGA-II + DCD + CE [45]	Best cost	–	608.12	–
	Best emission	–	0.1942	–

$$E(P) = \sum_{i=1}^{N} [10^{-2}(\alpha_i P_i^2 + \beta_i P_i + \gamma_i)], \tag{21}$$

and the item $\varepsilon_i \exp(\lambda_i P_i)$ is omitted. Totally, even the maximum value of best cost obtained by MHBA is smaller than the minimum values obtained by the other three algorithms, and all the four methods have nearly the "same" minimum emissions. It indicates that whether for the quality or for the stability of the best solutions, MHBA has an absolute advantage among the listed algorithms.

Based on the above analysis, MHBA has excellent performance in dealing with CEED problem for IEEE 30-bus system.

4.2. Case 2: simulation for the standard IEEE 118-bus system

The proposed MHBA is applied to the standard IEEE 118-bus system with 19 units in this subsection. The parameters including unit characteristics and coefficients (cost and emission) are taken from [44]. The unit characteristics contains ramp rate level, startup costs, shut down costs, active power output constraints, etc., and the load demand is 3668 MW. In this case, the number of population for MHBA is also set to 50. The minimum and maximum frequency of pulse emission rate are 0 and 0.01, respectively. The parameter r_d and threshold p for the random black hole model are 1 and 0.5, respectively, and the learning probability P_c is 0.1. The following simulations all include ramp rate limit in this case. For the comparison purpose, the simulation results without/with POZs are given separately in Sections 4.2.1 and 4.2.2, respectively. At last, all the aforementioned constraints in Section 2 are included in the simulation which is shown in Section 4.2.3.

4.2.1. No POZs are included in the simulation

Fig. 5 shows the POFs which have the best fuel cost and emission in ten runs. The best two extreme solutions in Fig. 5 are (10186.8, 5.5417) and (11433.3, 5.5117), respectively. The detailed comparison results including best fuel cost and best emission in ten runs are represented in Tables 4 and 5, respectively. In Table 4, the best fuel cost obtained by MHBA is 101186.8$/h which is much less than the other relative values. Accordingly, the best emission obtained by MHBA is 5.5417 ton/h which is also the smallest value among the listed emissions. In Table 5, the best value emission generated by MHBA is about 5.5117 ton/h and NSGA-II + DCD + CE acquires the best value. Although MHBA does not achieve the optimum value of best emission, but the difference is only 0.093 ton/h (the increased percentage is about 1.68%). By contrast, the difference best fuel cost between MHBA and NSGA-II + DCD + CE in Table 4 is about 1246.6$/h (the decreased percentage is about 12.28%). Hence, majority of the solutions generated with NSGA-II + DCD + CE are dominated by the solutions in Fig. 5. The best compromise solution can give the evidence. As shown Fig. 5, the best compromise solution obtained by MHBA is (10634.2, 5.5191), but for NSGA-II + DCD + CE, the solution is (16205.3, 5.7848) (see [45]). Obviously, MHBA achieves better compromise solution than NSGA-II + DCD + CE.

Table 4 also gives the comparison result of execution time. For

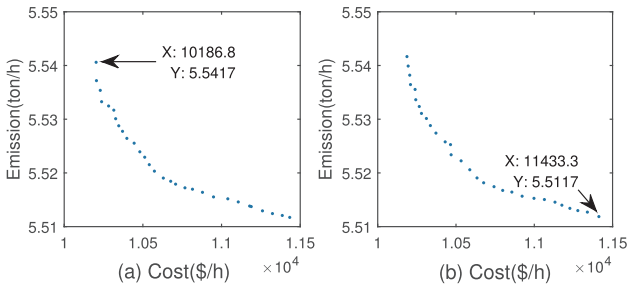

Fig. 5. (a) POF of the best fuel cost without POZs for case 2. (b) POF of the best emission without POZs for case 2.

Table 4
Best solutions of fuel cost in ten runs for case 2 without POZs (Power: MW, Cost: $/h, Emission: ton/h, Run time: s).

Items	MHBA	MNSGA -II [9]	NSGA -II [9]	RCGA [9]	NSGA-II + DCD [45]	NSGA-II + DCD + CE [45]
P_1	787.58	611.29	640.18	673.52	623.95	691.44
P_2	499.45	62.23	54.08	73.06	50.67	68.45
P_3	10.00	89.07	83.84	76.07	89.25	89.24
P_4	30.00	298.65	285.21	299.99	297.64	297.08
P_5	231.01	40.07	40.49	40.00	40.07	40.07
P_6	1.00	5.32	1.44	1.02	4.97	1.45
P_7	3.00	9.50	12.74	17.65	20.32	20.57
P_8	30.00	31.86	30.03	30.00	30.36	30.64
P_9	5.00	41.87	48.72	10.39	48.81	24.15
P_{10}	27.81	195.86	151.96	138.69	185.46	102.17
P_{11}	20.00	197.05	190.13	199.99	197.07	194.79
P_{12}	399.21	395.26	394.83	399.59	399.18	396.96
P_{13}	398.85	398.51	397.63	399.95	398.78	399.90
P_{14}	598.30	582.46	590.54	599.99	570.08	599.47
P_{15}	1.00	3.02	3.99	3.68	1.52	1.52
P_{16}	625.27	658.53	672.04	690.62	631.74	690.24
P_{17}	152.11	243.36	240.91	228.31	265.22	222.73
P_{18}	5.00	10.79	36.10	5.31	7.36	5.28
P_{19}	4	5.70	6.96	8.30	4.04	4.79
Loss	160.58	212.5	213.90	228.50	198.56	213.03
Cost	**10186.8**	11552.0	11577.5	11509.7	11451.2	11396.8
Emission	5.5417	13.7960	14.1910	14.9726	13.4788	15.0395
Run time	**104.797**	825.875	838.171	31806.1	806	1142

Table 5
Best solutions of emission in ten runs for case 2 without POZs (Power: MW, Cost: $/h, Emission: ton/h).

Items	MHBA	MNSGA -II [9]	NSGA -II [9]	RCGA [9]	NSGA-II + DCD + CE [45]	NSGA-II + DCD + CE [45]
P_1	299.12	330.36	314.74	310.33	3221.12	321.08
P_2	482.28	436.53	396.63	425.52	397.62	430.21
P_3	10.00	89.83	82.98	89.99	88.88	89.57
P_4	30.00	299.49	299.49	299.99	292.13	292.13
P_5	40.00	394.78	395.52	399.99	389.20	399.51
P_6	1.00	5.68	8.83	1.66	8.81	5.11
P_7	3.22	8.78	22.66	18.70	18.95	18.15
P_8	240.00	239.60	236.20	239.99	239.39	239.82
P_9	5.00	40.01	49.48	49.98	49.44	49.24
P_{10}	146.19	197.99	199.66	199.95	198.21	199.94
P_{11}	200.00	194.05	198.92	199.99	194.89	198.63
P_{12}	399.95	303.40	340.86	291.42	300.93	295.67
P_{13}	400.00	385.21	386.81	399.83	399.91	384.51
P_{14}	599.86	157.57	174.59	167.68	171.33	165.63
P_{15}	1.00	3.78	4.89	1.64	1.29	4.16
P_{16}	699.49	310.37	303.70	307.75	312.47	300.89
P_{17}	300.00	291.66	276.89	292.74	296.32	289.17
P_{18}	5.00	46.15	38.28	49.98	49.61	49.33
P_{19}	5.01	39.74	39.80	26.84	37.83	38.96
Loss	199.12	107.1	103	106.0	101.42	103.79
Cost	11433.0	18311.0	17993.4	18227.5	17948.6	18343.2
Emission	5.5117	5.5466	5.4950	5.4876	5.4451	**5.4230**

Table 6
Statistical results for the best fuel cost and emission with ten runs for case 2 without POZs (Cost: $/h, Emission: ton/h).

Algorithm	Items	Maximum	Minimum	Average
MHBA	Best cost	10226.3	10186.8	10205.2
	Best emission	5.5121	5.5117	5.5119
NSGA-II [45]	Best cost	–	11440.8	–
	Best emission	–	5.4164	–
NSGA-II + DCD [45]	Best cost	–	11451.2	–
	Best emission	–	5.4451	–
NSGA-II + DCD + CE [45]	Best cost	–	11396.8	–
	Best emission	–	5.4230	–

MHBA, the consumed time is about 104.797 s. But for the other five algorithms, the minimal execution time is about 806 s which is obtained by NSGA-II + DCD. The most time-consuming algorithm is RCGA whose consumed time exceeds 31806 s. Thanks to the usage of the random black hole model, MHBA can have such better performance in speed. For other algorithms, all the dimensions in a solution are updated simultaneously. But MHBA can realize the update for each single dimension in every solution (the schematic is shown in Algorithm 3) because of the integrating of random black hole model. This strategy is more suitable for high dimensional system. Moreover, the random black hole model is also helpful in enlarging global search ability and accelerating convergence speed. The current group best solution is treated as the base point of random black hole generated at each iteration. This is meaningful for individuals to find more accurate solutions, and the reason is given as follows:

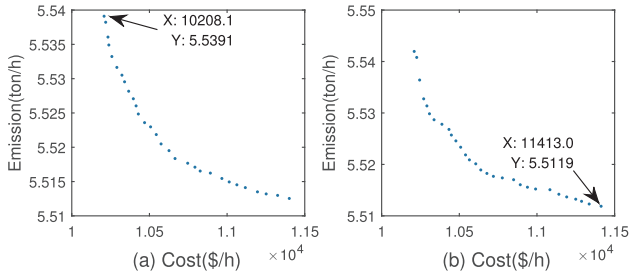

Fig. 6. (a) POF of the best fuel cost with POZs for case 2. (b) POF of the best emission with POZs for case 2.

① The search area is enlarged for the use of the effective radius r_d in random black hole model. An appropriate value of r_d is helpful not only in enlarging the search area but also in accelerating convergence speed.

② It helps to find more accurate solutions. If the current group best solution is a local optimal solution, the random black hole would help individuals escape from the local optima. But if the current group best solution is near to the real global optimum (although it is unknown), the random black hole model can help to execute a complete search around the current group best solution.

To further disclose the superiority of MHBA, Table 6 gives the statistical results for the best fuel cost and emission with the ten runs. The best cost values (maximum, minimum and average values) obtained by MHBA are smaller than all the minimum values of fuel cost generated by the other three algorithms.

Therefore, MHBA outperforms the other listed algorithms in all comparison items except the minimum emission for the IEEE 118-bus system.

4.2.2. *POZs are included in the simulation*

The parameter of POZs comes from [9], and all the other parameters are the same as in Section 4.2.1. The following comparison results are also based on ten runs.

Fig. 6 shows the two POFs which have best fuel cost and best emission including POZs. The best fuel cost is 10208.1$/h and the best emission is 5.5119 ton/h. Both the two values are a little bigger than the corresponding values in Fig. 5 for the effect of POZs. Table 7 shows the comparison results of best fuel cost with other algorithms. MHBA gets the optimal value of fuel cost in the listed algorithms. The decreased percentages compared with MNSGA-II, NSGA-II and RCGA are 16.6%, 26.0% and 14.2%, respectively. As for the run time, MHBA is much superior to other listed algorithms. The consumed time for MHBA is about 105.885 s, which is much smaller than the other algorithms. The best solutions of emission with other algorithms are shown in Table 8. For MHBA, the value of best emission is about 5.5119 which is also the smallest in the listed algorithms. Therefore, MHBA outperforms other listed algorithms in terms of the two best values.

To further show the superiority of MBHA, the statical results for the best cost and emission with ten run are given in Table 9. The minimum/average values of the best cost and emission are all a little bigger than the relative values as shown in Table 6 because of the existing of POZs. Even the maximum values of best fuel cost and emission in Table 9 are

Table 7
Best solutions of fuel cost in ten runs for case 2 with POZs (Power: MW, Cost: $/h, Emission: ton/h, Run time: s).

Items	MHBA	MNSGA-II [9]	NSGA-II [9]	RCGA [9]
P_1	831.62	661.11	652.05	825.00
P_2	406.22	158.57	300.50	150.00
P_3	10.00	68.77	66.82	80.99
P_4	30.08	299.34	232.64	229.98
P_5	235.76	41.29	101.62	40.00
P_6	1.00	8.75	8.78	1.00
P_7	3.00	6.27	18.62	22.98
P_8	104.19	31.94	30.60	30.00
P_9	5.00	39.28	32.01	39.99
P_{10}	20.00	196.55	122.00	132.35
P_{11}	20.00	159.66	88.37	199.99
P_{12}	363.83	391.21	322.58	324.88
P_{13}	398.63	399.68	383.36	399.99
P_{14}	599.17	433.54	555.77	562.95
P_{15}	1.00	1.31	2.91	1.00
P_{16}	698.46	652.24	666.42	549.97
P_{17}	100.00	285.50	217.14	224.88
P_{18}	6.38	15.17	8.09	5.00
P_{19}	4.00	7.08	33.09	4.00
Loss	170.33	189.32	170.93	157.1
Cost	**10208.1**	11904.1	12862.4	11655.8
Emission	5.5391	11.9724	13.0403	13.0098
Run time	**105.885**	1762.45	1781.69	63638.3

Table 8
Best solutions of emission in ten runs for case 2 with POZs (Power: MW, Cost: $/h, Emission: ton/h).

Items	MHBA	MNSGA-II [9]	NSGA-II [9]	RCGA [9]
P_1	303.59	316.79	311.37	300.00
P_2	484.82	452.19	386.74	450.00
P_3	10.01	68.53	89.76	89.99
P_4	30.00	246.66	174.62	249.99
P_5	40.30	347.02	348.12	388.01
P_6	1.30	9.38	9.80	9.99
P_7	3.00	8.51	22.99	22.99
P_8	240.00	238.16	234.40	239.96
P_9	6.53	49.80	39.64	499.99
P_{10}	136.17	199.96	199.98	199.99
P_{11}	200.00	199.18	199.44	199.99
P_{12}	400.00	279.95	350.61	250.41
P_{13}	400.00	399.67	399.96	372.41
P_{14}	600.00	157.96	220.42	149.54
P_{15}	1.00	1.78	3.89	4.994
P_{16}	700.00	451.47	451.07	450.00
P_{17}	300.00	282.65	289.00	255.32
P_{18}	5.69	45.12	5.23	49.99
P_{19}	4.00	19.04	31.43	39.99
Loss	198.42	105.90	100.56	105.70
Cost	11413.0	17541.7	16910.6	18240.6
Emission	**5.5119**	6.0496	6.3309	5.7111

Table 9
Statistical results for the best fuel cost and emission with ten runs for case 2 with POZs (Cost: $/h, Emission: ton/h).

Algorithm	Items	Maximum	Minimum	Average
MHBA	Best cost	10222.6	10208.1	10221.2
	Best emission	5.5150	5.5119	5.5126

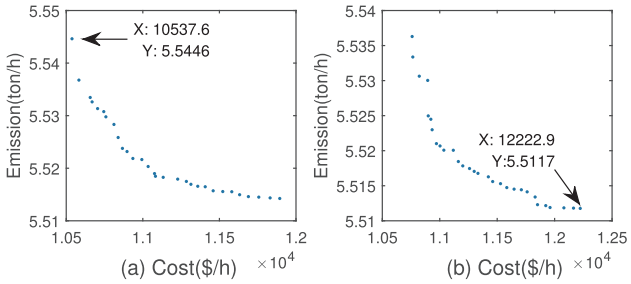

Fig. 7. (a) POF of the best fuel cost with all constraints for case 2. (b) POF of the best emission with all constraints for case 2.

Table 10
Best solutions of fuel cost in ten runs for case 2 with all constraints (Power: MW, Cost: $/h, Emission: ton/h, Run time: s).

Items	MHBA	MNSGA-II [9]	NSGA-II [9]	RCGA [9]
P_1	876.82	647.70	619.24	657.56
P_2	483.11	52.96	95.49	56.72
P_3	10.95	88.71	89.43	83.98
P_4	31.11	295.43	299.84	295.47
P_5	250.00	41.97	40.39	40.36
P_6	1.00	7.01	2.91	3.99
P_7	3.00	16.57	10.56	17.01
P_8	30.00	30.89	33.21	30.11
P_9	5.00	47.87	33.63	46.01
P_{10}	20.00	171.92	198.87	152.79
P_{11}	20.00	192.81	191.02	199.62
P_{12}	385.48	399.75	386.31	399.86
P_{13}	396.17	399.46	395.33	384.55
P_{14}	599.63	581.20	548.72	597.15
P_{15}	1.00	1.18	1.09	2.93
P_{16}	698.72	602.69	661.36	651.21
P_{17}	30.00	271.81	252.20	239.03
P_{18}	5.00	6.76	5.97	23.03
P_{19}	4.21	6.16	4.80	5.50
Loss	198.07	194.93	202.46	218.98
Cost	**10537.6**	11944.0	12043.8	12039.2
Emission	5.5446	13.5930	13.2770	14.2840
Run time	**109.664**	870.523	867.342	31938.32

smaller than the relative values obtained by other algorithms in Tables 7 and 8.

4.2.3. All the listed constraints are included in the simulation

Compared with Section 4.2.2, the valve point effects are included in the simulation and the parameters are taken from [9,54]. Other parameters are the same as in Section 4.2.2. Ten runs are also executed for this simulation.

Fig. 7 shows the POFs which have the best fuel cost and best emission. The best fuel cost is 10537.6$/h, which is a little larger than that in Fig. 6 (i.e., 10208.1$/h) because the valve point effects are

Table 11
Best solutions of emission in ten runs for case 2 with all constraints (Power: MW, Cost: $/h, Emission: ton/h).

Items	MHBA	MNSGA-II [9]	NSGA-II [9]	RCGA [9]
P_1	300.05	318.55	309.40	299.24
P_2	499.49	406.68	413.20	429.01
P_3	10.00	80.82	84.30	83.29
P_4	30.00	297.83	284.14	283.87
P_5	40.00	396.48	395.50	399.73
P_6	1.02	8.39	6.53	9.87
P_7	3.00	22.85	22.85	22.16
P_8	239.76	232.41	238.81	236.78
P_9	5.65	43.54	49.86	44.70
P_{10}	126.86	199.39	178.82	199.21
P_{11}	200.00	198.89	194.30	199.48
P_{12}	400.00	330.96	320.01	362.94
P_{13}	399.49	390.69	389.45	371.46
P_{14}	600.00	177.04	159.18	168.44
P_{15}	1.66	4.80	3.02	1.88
P_{16}	700.00	316.59	347.36	282.91
P_{17}	300.00	263.65	288.18	296.96
P_{18}	6.37	47.78	48.76	49.15
P_{19}	4.65	34.53	37.94	31.69
Loss	200.05	103.95	103.69	104.86
Cost	12222.9	18482.0	18533.6	18795.7
Emission	**5.5117**	5.5210	5.5390	5.5630

Table 12
Statistical results for the best fuel cost and emission with ten runs for case 2 with all constraints (Cost: $/h, Emission: ton/h).

Algorithm	Items	Maximum	Minimum	Average
MHBA	Best cost	10864.54	10537.64	10720.84
	Best emission	5.5142	5.5117	5.5126

included in the simulation. The best emission is 5.5117 ton/h, which is nearly the same as in Fig. 6 (i.e., 5.5119 ton/h).

Tables 10 and 11 show the comparison results with other algorithms for the best solutions of fuel cost and emission, respectively. It should be pointed out that the data in [9] is obtained without considering POZs. Even under this situation, MHBA gets the best values of fuel cost and emission compared with other listed algorithms. In Table 10, the optimal fuel cost obtained by MHBA is 10537.6$/h, and the minimum value by the other algorithms is 11944.0$/h. The decreased percentage is about 11.77%. In Table 11, the optimal emission obtained by MHBA is 5.1117 ton/h, which is also the smallest among the four algorithms. As for the run time, MHBA has obviously advantageous than other listed algorithms. In Table 10, the run time for MHBA is 109.664 s. For the other three algorithms, the smallest run time is 867.342 s, which is about 7.9 times than that obtained by MHBA.

Table 12 gives the statistical results for the best fuel cost and emission with ten runs. The maximum value of fuel cost is 10864.54$/h, which is even smaller than the best solution obtained by MNSGA-II (i.e., 11944.0$/h, see Table 10). The maximum value of emission generated by MHBA is 5.5142 ton/h, which is also the smallest compared with the best emissions obtained by the other three algorithms in Table 11. All these demonstrate the effectiveness of MHBA in solving CEED for IEEE 118-bus system considering practical constraints.

4.3. Case 3: simulation for the standard IEEE 300-bus system

The IEEE 300-bus system with 57 units is used in this subsection. The fuel cost coefficients, emission coefficients and active power output limits of units are all adapted from [44]. Other parameters of IEEE 300-bus system comply with MATPOWER. The emphasis here is to show the effectiveness of MHBA for large-scale system, so the constraints including ramp rate limit and POZs are omitted in this case, and the transmission line losses are assumed to be zero. The total load demand is 23525.85 MW. To better show the simulations, ten runs are also executed for this case. In this case, the effective radius r_d is treated as a piecewise parameter. At the steps of 1 to 200, r_d is set to 50, and at the rest of iteration, r_d is set to 1. Other parameters of RCBA are the same as in case 2.

Fig. 8 shows the POFs of best fuel cost and best emission with ten runs. The best two extreme solutions are (62879.2, 11.6701) and (66317.4, 11.5385), respectively. The detailed active power outputs of

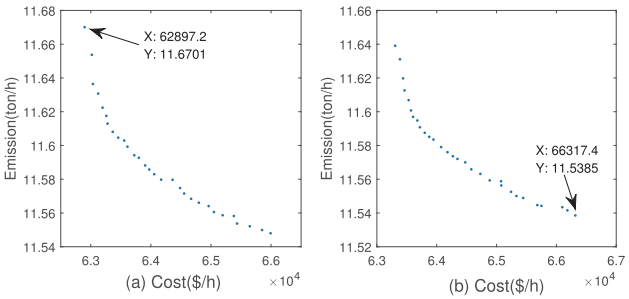

Fig. 8. (a) POF of the best fuel cost for case 3. (b) POF of the best emission for case 3.

Table 13
The best solution of fuel cost with ten runs for case 3 (Power: MW, Cost: $/h, Emission: ton/h, Run time: s).

Units	Output	Units	Output	Units	Output
P_1	464.1060	P_{20}	1191.9413	P_{39}	1238.3642
P_2	30.0111	P_{21}	600.0000	P_{40}	241.7455
P_3	158.9477	P_{22}	1927.5783	P_{41}	396.0250
P_4	20.5789	P_{23}	479.9002	P_{42}	373.7095
P_5	25.0000	P_{24}	302.8914	P_{43}	188.8349
P_6	1551.2870	P_{25}	20.5789	P_{44}	487.1919
P_7	278.3228	P_{26}	526.3353	P_{45}	556.6738
P_8	269.7550	P_{27}	229.4327	P_{46}	20.7548
P_9	751.8381	P_{28}	332.9978	P_{47}	846.4540
P_{10}	91.8085	P_{29}	372.9751	P_{48}	15.0789
P_{11}	180.9106	P_{30}	296.8753	P_{49}	159.1250
P_{12}	25.5789	P_{31}	686.1086	P_{50}	477.5703
P_{13}	446.9643	P_{32}	225.3648	P_{51}	398.7751
P_{14}	154.7756	P_{33}	610.4855	P_{52}	90.0360
P_{15}	225.7937	P_{34}	540.4389	P_{53}	1106.0333
P_{16}	222.9625	P_{35}	142.9897	P_{54}	715.8791
P_{17}	131.0865	P_{36}	94.6735	P_{55}	620.7908
P_{18}	188.8311	P_{37}	478.8570	P_{56}	21.4258
P_{19}	1134.5317	P_{38}	641.1964	P_{57}	21.2532
$\sum P_i$	24030.43	Loss	504.58		
Cost	62897.2	Emission	11.6701	Run time	265.118

the 57 units for the two extreme solutions are shown in Tables 13 and 14, respectively. The run time for IEEE 300-bus system is about 265 s, which is even much less than those for IEEE 118-system obtained by other algorithms. This also demonstrates the superiority of RCBA in terms of the random search efficiency. The loss in Tables 13 and 14 accounts for about 2.01% and 5.23% of the total active power output, respectively. Table 15 gives the statistical results for the best fuel cost and emission with ten runs. All the data shows that the CEED for IEEE 300-bus is well solved by RCBA.

In the following, we put the emphasis on the usage of an important parameter, that is, the effective radius r_d through IEEE 300-bus system. Generally, the value of r_d should be changed with different systems. If the search range of individuals is relatively large, r_d should be assigned with a relatively large value, and vice verse. For this case, several simulations with different values of r_d are performed to illustrate what value that r_d should have, and the simulation results are shown in Table 16.

Table 14
The best solution of emission with ten runs for case 3 (Power: MW, Cost: $/h, Emission: ton/h, Run time: s).

Units	Output	Units	Output	Units	Output
P_1	440.1843	P_{20}	1238.5322	P_{39}	1097.3666
P_2	30.4980	P_{21}	577.9914	P_{40}	251.6531
P_3	115.0420	P_{22}	1968.6719	P_{41}	407.5548
P_4	20.0000	P_{23}	592.6413	P_{42}	383.1900
P_5	27.0272	P_{24}	322.5295	P_{43}	191.9195
P_6	600.6554	P_{25}	109.2913	P_{44}	592.7593
P_7	274.5312	P_{26}	599.3657	P_{45}	581.4626
P_8	309.5829	P_{27}	247.0924	P_{46}	13.7000
P_9	774.1955	P_{28}	332.6852	P_{47}	1658.7119
P_{10}	69.1177	P_{29}	413.3995	P_{48}	23.5977
P_{11}	206.8483	P_{30}	332.1506	P_{49}	186.9400
P_{12}	93.1053	P_{31}	665.4951	P_{50}	435.6961
P_{13}	480.2329	P_{32}	258.2336	P_{51}	440.7719
P_{14}	220.6048	P_{33}	581.4698	P_{52}	127.4313
P_{15}	188.7268	P_{34}	695.8082	P_{53}	1075.0831
P_{16}	255.8392	P_{35}	192.2545	P_{54}	718.6377
P_{17}	98.1057	P_{36}	95.9989	P_{55}	615.7556
P_{18}	226.5371	P_{37}	589.8898	P_{56}	62.5584
P_{19}	967.8302	P_{38}	724.0515	P_{57}	24.1172
$\sum P_i$	24825.12	Loss	1299.27		
Cost	66317.4	Emission	11.5385	Run time	266.581

Table 15
Statistical results for the best fuel cost and emission with ten runs for case 3 without POZs (Cost: $/h, Emission: ton/h).

Algorithm	Items	Maximum	Minimum	Average
MHBA	Best cost	63411.2	62897.2	63149.5
	Best emission	11.5632	11.5385	11.5529

Table 16
The two extreme solutions of POF with different values of r_d for case 3 (Cost: $/h, Emission: ton/h).

r_d	0.001	0.1	1
Left	(63032.3, 11.6348)	(63179.0, 11.6729)	(63317.2, 11.6427)
Right	(65191.7, 11.5794)	(65098.8, 11.6115)	(65389.6, 11.5876)
r_d	20	50	100
Left	(63008.5, 11.6360)	(63156.7, 11.6409)	(62839.9, 11.6243)
Right	(66160.7, 11.5495)	(66156.9, 11.5509)	(65076.2, 11.5431)

In Table 16, the differences of fuel cost between the two extreme solutions are 2159.4$/h, 1919.0$/h and 2072.4$/h when r_d is 0.001, 0.1 and 1, respectively. But when r_d is set to 20, 50 and 100, the differences are 3152.2$/h, 3000.2$/h and 2237.2$/h, respectively. The former differences are all smaller than the latter, which clearly shows that a larger range of fuel cost is obtained with a relatively large effective radius. Meanwhile, the difference obtained with the value 100 of r_d is smaller than those with 20 and 50. And hence, it is reasonable for r_d to be in the range of (1, 100).

Fig. 9 shows the POFs with different values of r_d. Better smoothness is obtained in Fig. 9(a) and (b) than that in Fig. 9(c) or (d). This means that a relatively small value of r_d is beneficial to generate POF. The reason is that a relatively small search area is formed with a relatively small r_d. This helps perform a thorough search in the area by individuals. But if r_d is too small at the beginning of iteration, the search area is relatively small, which is harmful for random search.

Based on the above analysis, a piecewise manner is proposed for r_d. To obtain a relatively large search area, r_d should be assigned with a relatively large value. As iteration goes on, r_d should be decreased to an appropriate value. For this case, r_d is set to 50 at the steps of 1 to 200. After this, r_d is set to 1.

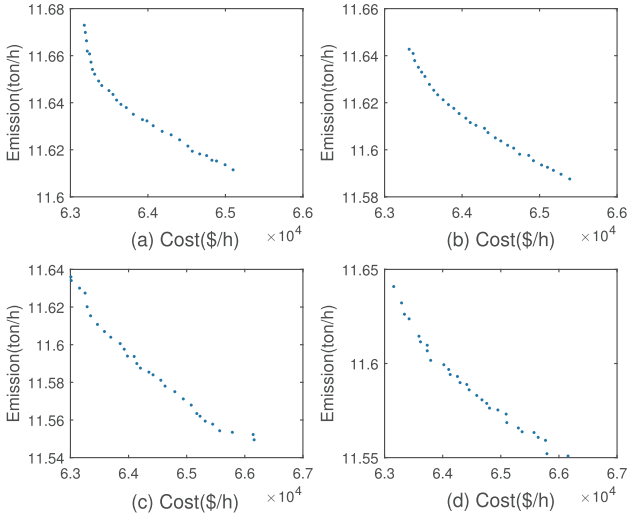

Fig. 9. (a) POF when r_d is 0.1. (b) POF when r_d is 1. (c) POF when r_d is 20. (d) POF when r_d is 50.

5. Concluding remarks

In this paper, a novel multiobjective hybrid bat algorithm has been presented and applied to CEED problem with IEEE 30-bus system, IEEE 118-bus system and IEEE 300-bus system. The comparison results show the superiority of MHBA for dealing with large-scale systems compared with other algorithms. To further enhance the performance of the proposed algorithm, for each solution x_i, the key parameter r_d can be assigned with different value, because the range of x_i is different generally. If the same value of r_d is used, the search area of partly individuals could be inappropriate. Moreover, the CEED is a bi-objective optimization problem. It is worth studying the optimization problems with more objectives. Renewable energies, such as wind power and solar energy, are widely used now, and hence are necessary to be included in CEED, which is left as an interesting future direction. The CEED problem studied in this paper is a static MOP, so another interesting direction is to study the dynamic economic/emission dispatch problem with the penetration of renewable energies and plug-in electric vehicles [47–49]. In addition, real-life case studies (see e.g., [50] and references therein) can be included in the simulation in future research. Finally, if the cost of emission in the trade market is considered [51–53], the objective function of emission would be reshaped. This will lead to a new direction.

Conflict of interest

None.

Acknowledgement

This work was supported in part by the National Natural Science Foundation of China under Grant 61325016, Grant 61374028 and Grant 61703237, in part by the Natural Science Foundation of Shandong Province under Grant ZR2017BF034, and in part by the China Postdoctoral Science Foundation Funded Project under Grant 2017M610424.

References

[1] Walters DC, Sheble GB. Genetic algorithm solution of economic dispatch with valve point loading. IEEE Trans Power Syst 1993;8(3):1325–32.
[2] Jayabarathi T, Raghunathan T, Adarsh BR, Suganthan PN. Economic dispatch using hybrid grey wolf optimizer. Energy 2016;111:630–41.
[3] Bayon L, Garu JM, Ruiz MM, Suarez PM. The exact solution of the environmental/economic dispatch problem. IEEE Trans Power Syst 2012;27(2):723–31.
[4] Rajan A, Malakar T. Optimum economic and emission dispatch using exchange market algorithm. Int J Elect Power Energy Syst 2016;82:545–60.
[5] Farag A, Al-Baiyat S, Cheng TC. Economic load dispatch multiobjective optimization procedures using linear programming techniques. IEEE Trans Power Syst 1995;10(2):731–8.
[6] Dhillon JS, Parti SC, Kothari DP. Stochastic economic emission load dispatch. Elect Power Syst Res 1993;26:186–97.
[7] Hsiao YT, Chiang HD, Liu CC, Chen YL. A computer package for optimal multi-objective VAR planning in large scale power systems. IEEE Trans Power Syst 1994;9(2):668–76.
[8] Venkatesh P, Gnanadass R, Padhy NP. Comparison and application of evolutionary programming techniques to combined economic emission dispatch with line flow constraints. IEEE Trans Power Syst 2003;18(2):688–97.
[9] Muthuswamy R, Krishnan M, Subramanian K, Subramanian B. Environmental and economic power dispatch of thermal generators using modified NSGA-II algorithm. Int Trans Electr Energ Syst 2015;25(8):1552–69.
[10] Khan NA, Sidhu GAS, Gao F. Optimizing combined emission economic dispatch for solar integrated power systems. IEEE Access 2016;4:3340–8.
[11] Abdelaziz AY, Ali ES, Abd Elazim SM. Implementation of flower pollination algorithm for solving economic load dispatch and combined economic emission dispatch problems in power systems. Energy 2016;101:506–18.
[12] Dhanalakshmi S, Kannan S, Mahadevan K, Baskar S. Application of modified NSGA-II algorithm to combined economic and emission dispatch problem. Int J Elect Power Energy Syst 2011;33(2):992–1002.
[13] Khan NA, Awan AB, Mahmood A, Razzaq S, Zafar A, Sidhu GAS. Combined emission economic dispatch of power system including solar photo voltaic generation. Energy Convers Manage 2015;92:82–91.
[14] Gong DW, Zhang Y, Qi CL. Environmental/economic power dispatch using a hybrid multi-objective optimization algorithm. Int J Elect Power Energy Syst 2010;32:607–14.
[15] Abdelaziz AY, Ali ES, Abd Elazim SM. Combined economic and emission dispatch solution using Flower Pollination Algorithm. Int J Elect Power Energy Syst 2016;80:264–74.
[16] Qu BY, Liang JJ, Zhu YS, Wang ZY, Suganthan PN. Economic emission dispatch problems with stochastic wind power using summation based multi-objective evolutionary algorithm. Inf Sci 2016;351:48–66.
[17] Naderi E, Azizivahed A, Narimani H, Fathi M. A comprehensive study of practical economic dispatch problems by anew hybrid evolutionary algorithm. Appl Soft Comput 2017;61:1186–206.
[18] Zhou JZ, Wang C, Li YZ, Wang P, Li CL, Lu P, et al. A multi-objective multi-population ant colony optimization for economic emission dispatch considering power system security. Appl Math Model 2017;45:684–704.
[19] Qu BY, Zhu YS, Jiao YC, Uw MY, Suganthan PN, Liang JJ. A survey on multi-objective evolutionary algorithms for the solution of the environmental/economic dispatch problems. Swarm Evol Comput 2018;38:1–11.
[20] Pandey HM, Chaudhary A, Mehrotra D. A comparative review of approaches to prevent premature convergence in GA. Appl Soft Comput 2014;24:1047–77.
[21] Tripathi PK, Bandyopadhyay S, Pal SK. Multi-objective particle swarm optimization with time variant inertia and acceleration coefficients. Inf Sci 2007;177:5033–49.
[22] Liu B, Wang L, Jin YH. An effective PSO–based memetic algorithm for flow shop scheduling. IEEE Trans Syst Man Cybern B Cybern 2007;37(1):18–27.
[23] Yang XS. A new metaheuristic bat-inspired algorithm. In: Gonzalez JR, editor. Nature inspired cooperative strategies for optimization (NISCO 2010). Studies in computational intelligence, vol. 28. Berlin: Springer; 2010. p. 65–74.
[24] Adarsh BR, Raghunathan T, Jayabarathi T, Yang XS. Economic dispatch using chaotic bat algorithm. Energy 2016;96:666–75.
[25] Ramesh B, Mohan VCJ, Reddy VCV. Application of bat algorithm for combined economic load and emission dispatch. Int J Electr Electron Eng Telecommun 2013;2(1):1–9.
[26] Niknam T, Azizipanah-Abarghooee R, Zare M, Bahmani-Firouzi B. Reserve constrained dynamic environmental/economic dispatch: a new multi-objective self-adaptive learning bat algorithm. IEEE Syst J 2013;7(4):763–76.
[27] Gonidakis D, Vlachos A. Bat algorithm approaches for solving the combined economic and emission dispatch problem. Int J Comput Appl 2015;124(1):1–7.
[28] Azizipanah-Abarghooee R, Niknam T. A new improved bat algorithm for fuzzy interactive multi-objective economic/emission dispatch with load and wind power uncertainty. In: Proc. of the 10th international FLINS conference; 2012. p. 388–93.
[29] Yang XS. Bat algorithm for multi-objective optimisation. Int J Bio-Inspired Comput 2011;3(5):267–74.
[30] Huang VL, Suganthan PN, Liang JJ. Comprehensive learning particle swarm optimizer for solving multiobjective optimization problems. Int J Intell Syst 2006;21(2):209–26.
[31] Xu JY, Wu CC, Yin YQ, Lin WC. An iterated local search for the multi-objective permutation flowshop scheduling problem with sequence-dependent setup times. Appl Soft Comput 2017;52:39–47.
[32] Yuan XH, Zhang BQ, Wang PT, Liang J, Yuan YB, Huang YH, et al. Multi-objective optimal power flow based on improved strength Pareto evolutionary algorithm. Energy 2017;122:70–82.
[33] Chaib AE, Bouchekara HREH, Mehasni R, Abido MA. Optimal power flow with emission and non-smooth cost functions using backtracking search optimization algorithm. Int J Elect Power Energy Syst 2016;81:64–77.
[34] Panigrahi BK, Pandi VR, Das Sa, Das Sw. Multiobjective fuzzy dominance based bacterial foraging algorithm to solve economic emission dispatch problem. Energy 2010;35:4761–70.
[35] Zhang JQ, Liu K, Tan Y, He XG. Random black hole particle swarm optimization and its application. In: Proc. IEEE int. conf. neural netw. signal process; 2008. p. 359–65.
[36] Zimmerman RD, Murillo-S¢nchez CE, Thomas RJ. MATPOWER: steady-state operations, planning and analysis tools for power systems research and education. IEEE Trans Power Syst 2011;26(1):12–9.
[37] Deb K, Pratap A, Agarwal S, Meyarivan T. A fast and elitist multiobjective genetic algorithm: NSGA-II. IEEE Trans Evol Comput 2002;6(2):182–97.
[38] Liang JJ, Qin AK, Suganthan PN, Baskar S. Comprehensive learning particle swarm optimizer for global optimization of multimodal functions. IEEE Trans Evol Comput 2006;10(3):281–95.
[39] Cheng S. Study on multi-objective optimization of distribution network with distributed generation [Ph.D. thesis]. Chongqing University; 2013.
[40] Suresh S, Lal S. Multilevel thresholding based on chaotic darwinian particle swarm optimization for segmentation of satellite images. Appl Soft Comput 2017;55:503–22.
[41] Li P, Xu D, Zhou ZY, Lee WJ, Zhao B. Stochastic optimal operation of microgrid based on chaotic binary particle swarm optimization. IEEE Trans Smart Grid 2016;7(1):66–73.
[42] Lu P, Zhou JZ, Zhang HF, Zhang R, Wang C. Chaotic differential bee colony optimization algorithm for dynamic economic dispatch problem with valve–point effects. Int J Elect Power Energy Syst 2014;62:130–43.
[43] Gandomi AH, Yang XS. Chaotic bat algorithm. J Comput Sci 2014;5(2):224–32.
[44] Karthikeyan SP, Palanisamy K, Rani C, Raglend IJ, Kothari DP. Security constrained unit commitment problem with operational, power flow and environmental constraints. WSEAS Trans Power Syst 2009;4(4):53–6.
[45] Dhanalakshmi S, Kannan S, Mahadevan K, Baskar S. Application of modified NSGA-II algorithm to combined economic and emission dispatch problem. Int J Elect Power Energy Syst 2011;33(4):992–1002.
[46] Dhillon JS, Parti SC, Kothari DP. Stochastic economic emission load dispatch. Electric Power Syst Res 1993;26:179–86.

[47] Yang ZL, Li K, Niu Q, Xue YS, Foley A. A self-learning TLBO based dynamic economic/environmental dispatch considering multiple plug-in electric vehicle loads. J Mod Power Syst Clean Energy 2014;2(4):298–307.
[48] Lokeshgupta B, Sivasubramani S. Multi-objective dynamic economic and emission dispatch with demand side management. Int J Elect Power Energy Syst 2018;97:334–43.
[49] Ma HP, Yang ZL, You PC, Fei MR. Multi-objective biogeography-based optimization for dynamic economic emission load dispatch considering plug-in electric vehicles charging. Energy 2017;135:101–11.
[50] Feng ZK, Niu WJ, Cheng CT, Wu XY. Peak operation of hydropower system with parallel technique and progressive optimality algorithm. Int J Elect Power Energy Syst 2018;94:267–75.
[51] Benidris M, Elsaiah S, Mitra J. An emission-constrained approach to power system expansion planning. Int J Elect Power Energy Syst 2016;81:78–86.
[52] Wen BY, Bai ZB, Wen FS. Environmental/economic dispatch considering emission benefit factor in the emission trading environment. Int J Energy Sector Manage 2011;5(3):407–15.
[53] Hossain M, Rastgoufard R, Rastgoufard P. Emission trading mechanism for environmental economic generation dispatch. In: Proc. IEEE green energy syst. conf.; 2016. p. 1–5.
[54] Ravi G, Chakrabarti R, Choudhuri S. Nonconvex economic dispatch with heuristic load patterns using improved fast evolutionary program. Electr Power Comp Syst 2006;34(1):37–45.